


## AUTHOR QUERY FORM

 ELSEVIER	<b>Journal: BBADIS</b>  <b>Article Number: 63856</b>	<b>Please e-mail or fax your responses and any corrections to:</b> <b>Prince, Don</b> <b>E-mail: <a href="mailto:Corrections.ESSD@elsevier.spitech.com">Corrections.ESSD@elsevier.spitech.com</a></b> <b>Fax: +1 619 699 6721</b>
---	--	--

Dear Author,

Please check your proof carefully and mark all corrections at the appropriate place in the proof (e.g., by using on-screen annotation in the PDF file) or compile them in a separate list. Note: if you opt to annotate the file with software other than Adobe Reader then please also highlight the appropriate place in the PDF file. To ensure fast publication of your paper please return your corrections within 48 hours.

For correction or revision of any artwork, please consult <http://www.elsevier.com/artworkinstructions>.

Any queries or remarks that have arisen during the processing of your manuscript are listed below and highlighted by flags in the proof. Click on the 'Q' link to go to the location in the proof.

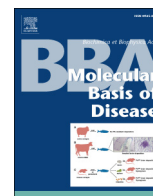
<b>Location in article</b>	<b>Query / Remark: <a href="#">click on the Q link to go</a> Please insert your reply or correction at the corresponding line in the proof</b>
<a href="#">Q1</a>	Please confirm that given names and surnames have been identified correctly.
<a href="#">Q2</a>	Please check if Table 1 data have been captured correctly and amend if necessary.
<a href="#">Q3</a>	This journal requires no abbreviations in the abstract where possible. Please check.
<a href="#">Q4</a>	Journal style requires a maximum of 6 keywords. Please check and provide the necessary correction.
<a href="#">Q5, Q6</a>	The accession number does not conform to the pattern for the accession number "NCBI GEO". Please check. <div data-bbox="639 1247 1133 1365" style="border: 1px solid black; padding: 5px; margin: 10px auto; width: fit-content;">             Please check this box if you have no corrections to make to the PDF file. <input type="checkbox"/> </div>

Thank you for your assistance.

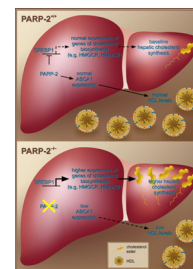


Contents lists available at ScienceDirect

## Biochimica et Biophysica Acta

journal homepage: [www.elsevier.com/locate/bbadis](http://www.elsevier.com/locate/bbadis)

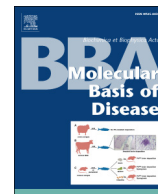
## Graphical abstract

**Deletion of PARP-2 induces hepatic cholesterol accumulation and decrease in HDL levels***Biochimica et Biophysica Acta xxx (2013) xxx – xxx*Magdolna Szántó<sup>a,b</sup>, Attila Brunyánszki<sup>a</sup>, Judit Márton<sup>b</sup>, György Vámosi<sup>c</sup>, Lilla Nagy<sup>b</sup>, Tamás Fodor<sup>b</sup>, Borbála Kiss<sup>d</sup>,  
László Virág<sup>a,b</sup>, Pál Gergely<sup>b</sup>, Péter Bai<sup>a,b,\*</sup><sup>a</sup> MTA-DE Cell Biology and Signaling Research Group of the Hungarian Academy of Sciences, 4032 Debrecen, Hungary<sup>b</sup> Department of Medical Chemistry, University of Debrecen, 4032 Debrecen, Hungary<sup>c</sup> Department of Biophysics and Cell Biology, University of Debrecen, 4032 Debrecen, Hungary<sup>d</sup> Department of Dermatology, Medical and Health Science Center, University of Debrecen, 4032 Debrecen, Hungary



Contents lists available at ScienceDirect

## Biochimica et Biophysica Acta

journal homepage: [www.elsevier.com/locate/bbadis](http://www.elsevier.com/locate/bbadis)

## Highlights

**Deletion of PARP-2 induces hepatic cholesterol accumulation and decrease in HDL levels***Biochimica et Biophysica Acta xxx (2013) xxx – xxx*Magdolna Szántó<sup>a,b</sup>, Attila Brunyánszki<sup>a</sup>, Judit Márton<sup>b</sup>, György Vámosi<sup>c</sup>, Lilla Nagy<sup>b</sup>, Tamás Fodor<sup>b</sup>, Borbála Kiss<sup>d</sup>, László Virág<sup>a,b</sup>, Pál Gergely<sup>b</sup>, Péter Bai<sup>a,b,\*</sup><sup>a</sup> MTA-DE Cell Biology and Signaling Research Group of the Hungarian Academy of Sciences, 4032 Debrecen, Hungary<sup>b</sup> Department of Medical Chemistry, University of Debrecen, 4032 Debrecen, Hungary<sup>c</sup> Department of Biophysics and Cell Biology, University of Debrecen, 4032 Debrecen, Hungary<sup>d</sup> Department of Dermatology, Medical and Health Science Center, University of Debrecen, 4032 Debrecen, Hungary

- Deletion of PARP-2 leads to hepatic cholesterol accumulation and reduced HDL level.
- Knockdown of PARP-2 enhances the expression of SREBP1 and SREBP1-dependent genes.
- The suppression of SREBP1 expression depends on the enzymatic activation of PARP-2.
- The deletion of PARP-2 decreases the expression of ABCA1.
- Lower ABCA1 protein level is a likely explanation for reduced HDL levels.

Supplementary Table 1. Primers for RT-qPCR. Abbreviations in the text. Supplementary Table 2. Primers for ChIP. Supplementary Table 3. Dysregulated genes in scPARP-2 vs. shPARP-2 HepG2 cells.

Fig. S1 PARP-2 knockdown leads to higher expression of SREBP1-dependent genes. (A–B) The Western blots in Fig. 3C were subjected to densitometry using the Image J software and densitometry data is plotted. (C–D) The Western blots in Fig. 3D were subjected to densitometry using the Image J software and densitometry data is plotted. \* and \*\* indicate statistically significant differences between scPARP-2 HepG2 cells/PARP-2<sup>+/+</sup> mice and shPARP-2 HepG2 cells/PARP-2<sup>-/-</sup> mice at  $p < 0.05$  and  $p < 0.01$ , respectively. In panels C and D error is given as SEM. Abbreviations are in the text.

Fig. S2 PARP-2 deletion reduces ABCA1 expression in cells and in vivo. (A) The Western blot in Fig. 5A was subjected to densitometry using the Image J software and densitometry data is plotted. (B) The Western blots in Fig. 5B were subjected to densitometry using the Image J software and densitometry data is plotted. \* indicates statistically significant difference between scPARP-2 HepG2 cells/PARP-2<sup>+/+</sup> mice and shPARP-2 HepG2 cells/PARP-2<sup>-/-</sup> mice at  $p < 0.05$ . In panel B error is given as SEM. Abbreviations are in the text.



## 1 Deletion of PARP-2 induces hepatic cholesterol accumulation and 2 decrease in HDL levels

Q1 **Magdolna Szántó<sup>a,b</sup>, Attila Brunyánszki<sup>a</sup>, Judit Márton<sup>b</sup>, György Vámosi<sup>c</sup>, Lilla Nagy<sup>b</sup>, Tamás Fodor<sup>b</sup>,  
4 Borbála Kiss<sup>d</sup>, László Virág<sup>a,b</sup>, Pál Gergely<sup>b</sup>, Péter Bai<sup>a,b,\*</sup>**

5 <sup>a</sup> MTA-DE Cell Biology and Signaling Research Group of the Hungarian Academy of Sciences, 4032 Debrecen, Hungary

6 <sup>b</sup> Department of Medical Chemistry, University of Debrecen, 4032 Debrecen, Hungary

7 <sup>c</sup> Department of Biophysics and Cell Biology, University of Debrecen, 4032 Debrecen, Hungary

8 <sup>d</sup> Department of Dermatology, Medical and Health Science Center, University of Debrecen, 4032 Debrecen, Hungary

### ARTICLE INFO

#### Article history:

11 Received 15 July 2013

12 Received in revised form 7 December 2013

13 Accepted 13 December 2013

14 Available online xxxx

#### Keywords:

19 PARP-2  
20 ARTD2  
21 SREBP1  
22 Cholesterol  
23 Liver  
24 HDL  
25 LDL  
26 Lipoprotein  
27 ABCA1  
28 UPF1069  
29 PARP inhibitor

### ABSTRACT

Poly(ADP-ribose) polymerase-2 (PARP-2) is acknowledged as a DNA repair enzyme. However, recent investigations have attributed unique roles to PARP-2 in metabolic regulation in the liver. We assessed changes in hepatic lipid homeostasis upon the deletion of PARP-2 and found that cholesterol levels were higher in PARP-2<sup>-/-</sup> mice as compared to wild-type littermates. To uncover the molecular background, we analyzed changes in steady-state mRNA levels upon the knockdown of PARP-2 in HepG2 cells and in murine liver that revealed higher expression of sterol-regulatory element binding protein (SREBP)-1 dependent genes. We demonstrated that PARP-2 is a suppressor of the SREBP1 promoter, and the suppression of the SREBP1 gene depends on the enzymatic activation of PARP-2. Consequently, the knockdown of PARP-2 enhances SREBP1 expression that in turn induces the genes driven by SREBP1 culminating in higher hepatic cholesterol content. We did not detect hypercholesterolemia, higher fecal cholesterol content or increase in serum LDL, although serum HDL levels decreased in the PARP-2<sup>-/-</sup> mice. In cells and mice where PARP-2 was deleted we observed decreased ABCA1 mRNA and protein expression that is probably linked to lower HDL levels. In our current study we show that PARP-2 impacts on hepatic and systemic cholesterol homeostasis. Furthermore, the depletion of PARP-2 leads to lower HDL levels which represent a risk factor to cardiovascular diseases.

© 2013 Published by Elsevier B.V.

### 1. Introduction

Poly(ADP-ribose) polymerase (PARP)-2 (also known as ARTD2) belongs to the PARP superfamily [1]. PARP-2 binds to DNA nicks and abnormal DNA structures through the SAP motif on its N-terminus [2] that activates PARP-2. Active PARP-2 cleaves NAD<sup>+</sup> to form poly(ADP-ribose) polymers attached to itself and to other acceptor proteins [1,3], however to date the proteins poly(ADP-ribosyl)ated by PARP-2 are poorly mapped.

PARP-2 participates in a plethora of processes such as DNA repair and genome surveillance, spermatogenesis, T cell maturation, inflammation and mediates oxidative injury [4]. PARP-2 was recently identified as a metabolic transcriptional regulator by influencing the activity of thyroid transcription factor 1, peroxisome proliferator activated receptor- $\gamma$  (PPARG), pancreatic and duodenal homeobox 1 (pdx-1) and SIRT1 [5–7]. Through these transcription factors PARP-2 regulates metabolism in white adipose tissue (WAT), pancreatic beta cells, skeletal muscle and liver [5,6]. Partial deletion of PARP-2 decreases PPARG and pdx-1 activity, which hampers WAT and beta cell function [5,6]. In skeletal muscle and liver the knockdown of PARP-2 induced SIRT1 expression and activity that consequently resulted in the

**Abbreviations:** ABCA1, adenosine triphosphate-binding cassette transporter A1; ACACA, cetyl-CoA carboxylase alpha; ACLY, ATP citrate lyase; ACOX2, acyl-CoA oxidase 2; ARTD2, ADP-ribosyl transferase diphtheria toxin-like 2; cyp51A1, cytochrome P450, family 51 subfamily A, polypeptide 1; CYP39A1, cytochrome P450, family 39, subfamily A, polypeptide 1; EGR-1, early growth response protein-1; ER $\alpha$ , estrogen receptor  $\alpha$ ; FABP1, fatty acid binding protein-1; FADS2, fatty acid desaturase 2; FASN, fatty acid synthase; FDPS, farnesyl diphosphate synthase; FOXO1, forkhead box protein O1; HDAC, histone deacetylase; HMGCR, 3-hydroxy-3-methylglutaryl (HMG)-CoA reductase; HMGCS1, 3-hydroxy-3-methylglutaryl (HMG)-CoA synthase 1 (cytoplasmic); HNF-4, hepatocyte nuclear factor 4; HP1 $\alpha$ , heterochromatin protein 1; K19, keratin 19; LDLR, LDL receptor; LIPA, lipase A; LIPG, endothelial lipase; LXR, liver X receptor; ME2, malic enzyme 2; MTTP, microsomal triglyceride transfer protein; PARP, poly(ADP-ribose) polymerase; Pdx-1, pancreatic and duodenal homeobox 1; PGC-1 $\alpha$ , peroxisome proliferator activated receptor cofactor-1 $\alpha$ ; PPARG, peroxisome proliferator activated receptor- $\gamma$ ; SCD, stearoyl-CoA delta-9-desaturase; sp1, specificity protein 1; SREBP, sterol regulatory element-binding protein; TIF1 $\beta$ , tripartite motif containing 28; WAT, white adipose tissue

\* Corresponding author at: Dept. of Medical Chemistry, University of Debrecen, Nagyterdei krt. 98. Pf. 7, H-4032 Debrecen, Hungary. Tel.: +36 52 412 345; fax: +36 52 412 566.

E-mail address: [baip@med.unideb.hu](mailto:baip@med.unideb.hu) (P. Bai).

deacetylation of downstream SIRT1 targets such as FOXO1 (forkhead box protein 1) or peroxisome proliferator activated receptor cofactor-1 $\alpha$  (PGC-1 $\alpha$ ). Deacetylation of these cofactors by SIRT1 leads to increased expression of genes involved in mitochondrial biogenesis leading to enhanced fatty acid oxidation [5].

Although several PARP isoforms were shown to influence metabolic processes, only PARP-2 was identified to regulate hepatic metabolism [8] (hepatic fatty acid accumulation upon the deletion of PARP-1 does not seem to stem from changes in hepatic metabolism [8–10]). The unique hepatic action of PARP-2 prompted us to assess in detail the role of PARP-2 in the regulation of lipid metabolism in the liver.

## 2. Materials and methods

### 2.1. Chemicals

All chemicals, including UPF1069, were from Sigma-Aldrich (St. Louis, USA) unless stated otherwise.

### 2.2. Cell culture

HepG2 human hepatocarcinoma cells were obtained from ATCC and were cultured in DMEM (1 g/L glucose, 10% FCS and for the selection of transduced cells 0.25  $\mu$ g/mL puromycin). PARP-2 silencing was performed using the same lentiviral constructs as in [5]. For silencing we employed constructs harboring a PARP-2 specific shPARP-2 small hairpin sequence or an unspecific scPARP-2 (scrambled) shRNA. The constructs were delivered to HepG2 cells via lentiviral particles (Sigma) using 40 MOI lentiviruses, and then puromycin-resistant cells were selected giving rise to PARP-2 silenced shPARP-2 HepG2 and control scPARP-2 HepG2 cell.

### 2.3. Animal studies

All animal experiments were carried out conforming to the national, EU and PHS ethical guidelines and were authorized by the Institutional Animal Care and Use Committee at the University of Debrecen (7/2010 DE MÁB). Homozygous male *PARP-2*<sup>-/-</sup> and littermate *PARP-2*<sup>+/+</sup> mice [11] derived from heterozygous crossings were kept in a 12/12 h dark-light cycle with ad libitum access to water and food (10 kcal% of fat, SAFE, Augy, France). Animals were sacrificed after 6 h of fasting (always in the same time, 12:00 p.m.), and tissues were collected and processed as specified.

### 2.4. Biochemical assays

Cholesterol and phospholipids in HepG2 cells, in liver and in fecal samples were determined by biochemical techniques after Floch extraction using kits from *Diagnosztikum* (Budapest, Hungary) and WAKO (Richmond, VA, USA). Serum cholesterol, LDL and HDL were determined using commercial kits from *Diagnosztikum*.

### 2.5. SDS-PAGE, Western blotting

Protein extraction, SDS-PAGE and Western blotting were performed as in [5]. Blots were probed with the following antibodies: SREBP1, SREBP2 (both 1:1000, Santa Cruz, Santa Cruz, CA, USA), HMGCS1, HMGCR, ABCA1 (1:1000, Abcam, Cambridge, UK), anti-poly(ADP-ribose) (mouse monoclonal antibody, 10H, Axxora, Lausen, Switzerland), actin (1:1000, Sigma) and PARP-2 (1:1000, Alexis, Lausen, Switzerland). Blots were quantified using the Image J software, then densitometry data were analyzed by statistical methods.

### 2.6. Cell fractionation

scPARP-2 and shPARP-2 HepG2 cells were pelleted by mild centrifugation at 4 °C at 1500 rpm for 3 min. The pellets were homogenized with five volumes of homogenization buffer (0.5 M sucrose, 20 mM HEPES pH 7.5, 1 mM EDTA, 1 mM EGTA and protease inhibitors) on ice and then Nonidet P-40 was added to a final concentration of 0.5%. The lysates were kept on ice and vortexed several times. Lysates were centrifuged at 8000  $\times$ g at 4 °C for 15 min. The supernatants were considered as cytosolic fractions. The pellets containing the nuclei were resuspended in four volumes of a buffer containing 0.35 M sucrose, 10 mM HEPES pH 7.9, 3.3 mM MgCl<sub>2</sub>, 10 mM KCl, 0.5 mM DTT and protease inhibitors. The suspensions were then sonicated on ice for 30 s, and the sonicated suspensions were used as nuclear fractions.

### 2.7. Immunocytochemistry and confocal microscopy

Confocal microscopic imaging was carried out at the Molecular Cell Analysis Core Facility at the University of Debrecen. For immunodetection of SREBP1 and SREBP2  $5 \times 10^5$  cells were seeded in each well of u-Slide 8 well chamber (ibidi, Munich, Germany). Cells were stained with an anti-SREBP1 or an anti-SREBP2 antibody (both in 1:50, Santa Cruz, Santa Cruz, CA, USA) antibody using the protocol described in [12]. Streptavidin-Alexa 488 conjugated secondary antibody was used at a dilution of 1:300 (60 min at room temperature). Nuclei were counterstained with propidium iodide (1  $\mu$ g/ml). An Olympus FV1000 confocal laser scanning microscope equipped with an UPLSAPO 60 $\times$  oil immersion objective (NA 1.35) was used to collect stacks of  $512 \times 512$  pixel optical slices with a z-step size of 500 nm. Alexa 488 (marking SREBP1 and SREBP2) and PI (labeling the nucleus) were excited at 488 and 543 nm, and detected between 500–300 and 555–655 nm, respectively. The pinhole was set to 120  $\mu$ m. The ratio of SREBP1 and SREBP2 concentrations within the nucleus and the cytoplasm was estimated from fluorescence intensities in these compartments. For analysis the brightest optical slice was selected from each cell. Separate regions of interest containing the nucleus and cytoplasmic areas were drawn by using the FluoView 3.0 software, and mean fluorescence intensities per pixel within the regions of interest were calculated. Background fluorescence was determined from cells incubated with the secondary antibody alone. The ratio of background-corrected intensities of nuclear to cytoplasmic intensities was calculated for ~10 cells in each sample. This ratio is proportional to the ratio of antibody (i.e. SREBP1/SREBP2) concentrations within these cellular compartments. Ratios measured for control and knockdown samples were compared by Student's t-tests.

### 2.8. DNA constructs and luciferase activity measurement

pGL2-SREBP1c-2600luc SREBP1 promoter was described previously [13], the luciferase reporter plasmid harboring the promoter of ABCA1 (pLightSwitch\_Prom-ABCA1) was from Switchgear Genomics (Menlo Park, CA, USA). PARP-2 mediated transactivation was determined in reporter assays as in [5]. Briefly,  $1 \times 10^5$  scPARP-2 and shPARP-2 HepG2 cells were seeded in 6 well plates. The following day cells were transfected with 2.5  $\mu$ g pGL2-SREBP1c-2600luc/pLightSwitch\_Prom-ABCA1 and 0.5  $\mu$ g  $\beta$ -galactosidase expression plasmid (pCMV- $\beta$ gal) using JetPEI (PolyPlus, Strasbourg, France). After 24 h cells were washed with PBS, scraped and stored at -80 °C. Luciferase assay was carried out by standard procedures. Luciferase activity was normalized to  $\beta$ -galactosidase activity.

### 2.9. Microarray experiments and validation

Total RNA was extracted from HepG2 cells using the RNeasy Mini Kit (Qiagen). RNA integrity was checked on Agilent Bioanalyser 2100 (Agilent Technologies), RNA samples with >9.0 RIN value were used in

the further experiments. NanoDrop ND-1000 was used to determine RNA concentration.

Global expression pattern was analyzed on Affymetrix GeneChip Human Gene 1.0 ST arrays. Ambion WT Expression Kit (Life Technologies, Hungary) and GeneChip WT Terminal Labelling and Control Kit (Affymetrix) were used for amplifying and labeling 250 ng of total RNA samples. Samples were hybridized at 45 °C for 16 h and then standard washing protocol was performed using Affymetrix GeneChip Fluidics Station 450, the arrays were scanned on GeneChip Scanner 7G (Affymetrix). RNA labeling and hybridization were processed by UD-GenoMed Medical Genomic Technologies Ltd. (Debrecen, Hungary).

Upon analysis low values (<500) were omitted as no, or low expressions of genes and the rest were normalized. The respective values for each gene were compared (shPARP-2 HepG2 vs. scPARP-2 HepG2 cells) using an unpaired t-test after Bonferroni correction and  $p < 0.05$  was considered as significant. Dysregulated genes were analyzed using the BINGO software of Cytoscape in order to classify the genes into biochemical pathways and functions. Hits were verified in RT-qPCR reactions. Raw and processed data is uploaded to NCBI GEO (accession No. 16716091).

### 2.10. RT-qPCR and chromatin immunoprecipitation

cdNA synthesis and RT-qPCR, were performed as described in [14], and primers are summarized in Supplementary Table 1. Chromatin immunoprecipitation was performed as in [14], and primers are summarized in Supplementary Table 2.

### 2.11. Statistical analysis

Statistical analysis of the microarray experiments was described above. In other cases, statistical significance was determined using Student's t-test. Error bars represent SD unless stated otherwise.

## 3. Results

### 3.1. Depletion of PARP-2 induces hepatic cholesterol levels and lowers serum HDL

Our previous study already showed that the deletion of PARP-2 leads to lower triglyceride levels in the liver due to higher mitochondrial activation through SIRT1 [5]. As an extension to that observation we analyzed the cholesterol and phospholipid levels in the livers of PARP-2<sup>+/+</sup> and PARP-2<sup>-/-</sup> mice (Fig. 1A–B). Hepatic cholesterol levels were higher in PARP-2<sup>-/-</sup> mice, primarily esterified cholesterol showed significant accumulation, while hepatic phospholipid levels were left unchanged (Fig. 1A–B). Next we verified whether hepatic cholesterol overproduction leads to higher cholesterol levels elsewhere too, but we did not observe higher cholesterol levels either in the faces (Fig. 1C) or in the serum (Fig. 1D). To our surprise, further analysis revealed that while LDL levels remained unchanged, HDL levels decreased in the PARP-2<sup>-/-</sup> mice (Fig. 1E). We set out to analyze the molecular background of increased hepatic cholesterol and lower HDL levels. To that end we created HepG2 cells in which PARP-2 was partially deleted.

### 3.2. Depletion of PARP-2 regulates gene expression in HepG2 cells and induces SREBP1-dependent genes

HepG2 cells were transduced with an shRNA construct directed against PARP-2 (sh) or its scrambled (sc) control, giving rise to shPARP-2 and scPARP-2 HepG2 cells, respectively. Transduction with the specific shRNA reduced PARP-2 mRNA and protein expression to 50% (Fig. 2A–B). Furthermore, the depletion of PARP-2 induced the cholesterol levels in the shPARP-2 HepG2 cells (Fig. 2C) similarly to the situation in the liver of the PARP-2<sup>-/-</sup> mice. Next we compared the steady state mRNA levels of the two cell lines in microarray experiments. We have detected the dysregulation of 616 genes (change in expression  $> +/ - 1.5$ ), the majority of which were downregulated in shPARP-2 HepG2 cells compared to scPARP-2 HepG2 cells (460

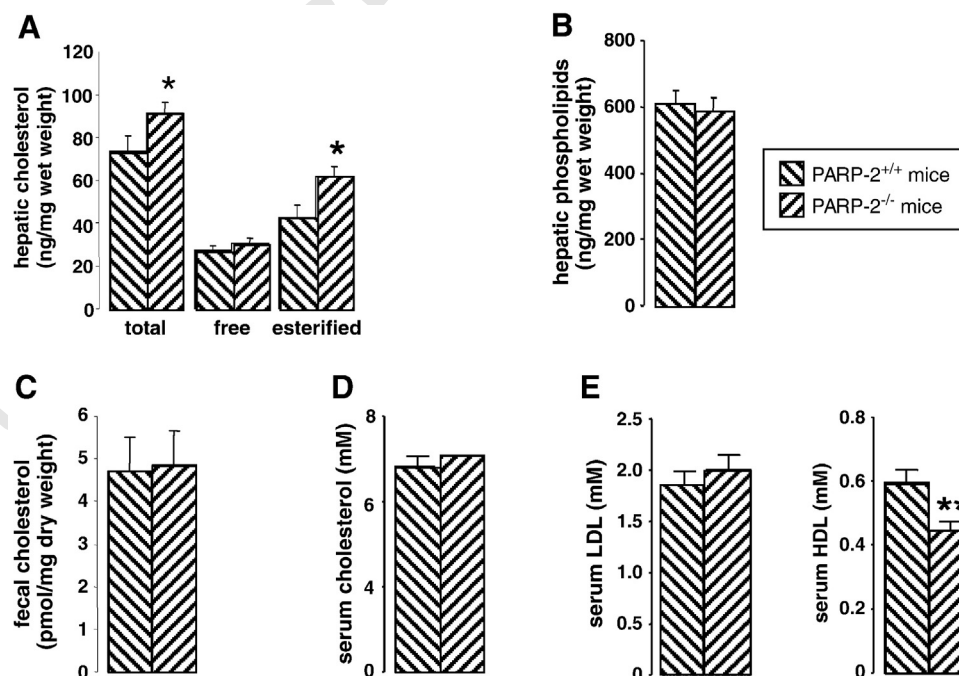
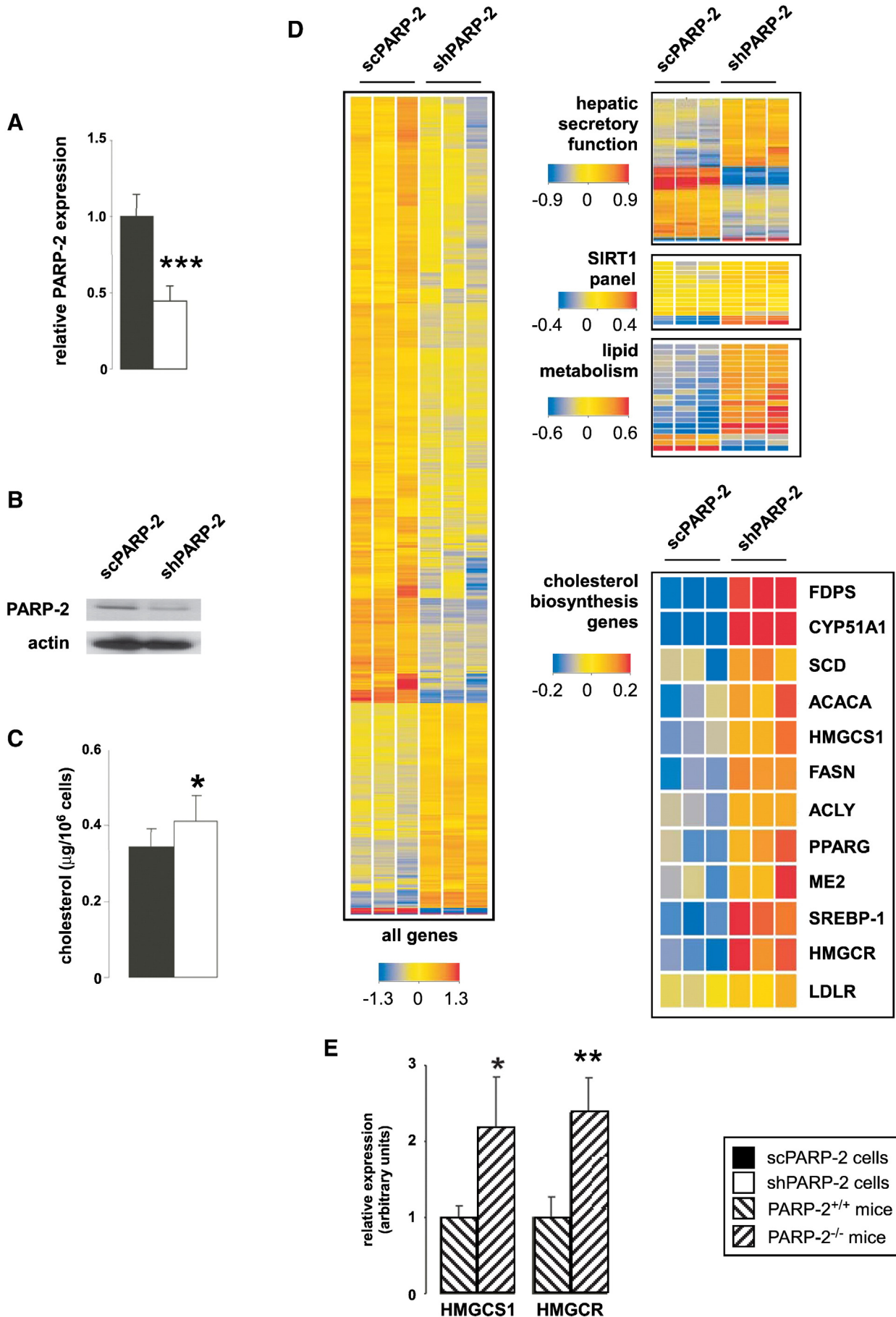


**Fig. 1.** Deletion of PARP-2 leads to higher hepatic cholesterol and lower serum HDL levels in vivo. (A–E) Liver cholesterol (A) and phospholipid (B) content, fecal (C) and serum (D) cholesterol, serum LDL and HDL (E) levels were determined in PARP-2<sup>+/+</sup> and PARP-2<sup>-/-</sup> mice (n = 7/6, age 6 months). \* and \*\* indicate statistically significant differences between PARP-2<sup>+/+</sup> and PARP-2<sup>-/-</sup> mice at  $p < 0.05$  and  $p < 0.01$ , respectively. Error is given as SEM.





**Q2** t1.1 **Table 1**  
 t1.2 Functional grouping of dysregulated genes in scPARP-2 vs. shPARP-2 HepG2 cells.  
 t1.3 Those genes are shown which had a change in expression of 1.5, or larger. \*, \*\* and \*\*\*  
 t1.4 indicate statistically significant differences between scPARP-2 cells and shPARP-2 cells at  
 t1.5  $p < 0.05$ ,  $p < 0.01$  and  $p < 0.001$ , respectively.

t1.6	Function	Upregulated genes		Downregulated genes		
		Name	Fold	Name	Fold	
t1.7						
t1.8	Lipid homeostasis	ACOX2	1.69***	ANXA1	-3.84***	
t1.9		ANGPTL3	1.90***	OSBPL10	-1.62***	
t1.10		APOM	1.75***	SERPINA3	-1.55***	
t1.11		CYP7A1	2.37***			
t1.12		CYP39A1	1.68***			
t1.13		ELOVL2	1.59***			
t1.14		FABP1	2.93***			
t1.15		FADS2	1.59***			
t1.16		LIPA	1.50***			
t1.17		LIPG	1.67***			
t1.18		MTTP	1.95***			
t1.19		PCSK9	1.59***			
t1.20		PPARGC1A	1.94***			
t1.21		SULT2A1	1.52***			
t1.22		TTPA	1.56***			
t1.23		UGT2B4	1.74***			
t1.24		Hepatic secretory functions	CCL16	1.84***	ADAM19	-2.69***
t1.25			CCL20	1.55***	ANXA1	-3.84***
t1.26			CPB2	1.88***	CAPN2	-1.62***
t1.27			CPN1	2.02***	CPA4	-1.96***
t1.28	CSF3R		1.51***	CPA6	-2.78***	
t1.29	C1R		1.71***	CTSE	-2.82***	
t1.30	C1S		2.02***	CD58	-1.53***	
t1.31	C2		1.50***	DPEP1	-1.81***	
t1.32	C5		1.85***	FURIN	-1.53***	
t1.33	C8A		1.84***	IL8	-1.65***	
t1.34	FGA		1.75***	KLRC3	-1.56***	
t1.35	FGG		1.69***	KLK6	-3.86***	
t1.36	F13B		1.63***	MALT1	-1.55***	
t1.37	HP		2.13***	MMP1	-1.56***	
t1.38	HPR		2.04***	NCF2	-1.74***	
t1.39	IFIT5		1.64***	PLAT	-1.75***	
t1.40	IFITM3		1.53***	PLAU	-2.08***	
t1.41	IL1R1		1.53***	PLAUR	-1.59***	
t1.42	KNG1		1.82***	PRF1	-1.89***	
t1.43	MASP1		1.54***	PRSS23	-2.08***	
t1.44	MASP2		1.59***	QPCT	-2.39***	
t1.45	MBL2		1.56***	SEMA3C	-2.14***	
t1.46	MEP1A		7.92***	SERPINA3	-1.55***	
t1.47	PCSK9		1.59***	SERPINE1	-2.54***	
t1.48	PRCP		1.54***	SERPINE2	-2.29***	
t1.49	SERPINF2		1.59***	SPP1	-1.59***	
t1.50	SERPING1		2.15***	TNFRSF9	-3.45***	
t1.51	TNFSF10	2.06***	TNFSF15	-1.68***		

238 down vs. 156 upregulated genes) (Fig. 2D, Supplementary Table 3.). Previous studies have already linked PARP-2 to transcription [5–7,15–18], however such widespread effect on gene expression was unexpected. We have observed altered expression in the following groups of genes: hepatic secreted proteins (proteins involved in blood coagulation and immune response), SIRT-1 regulated genes, lipid metabolism genes and SREBP-dependent genes (Fig. 2D, Table 1).

264 Higher expression of the SIRT1-dependent genes was in line with our previous observations [5,14] that validated the current study. The expression of genes involved in lipid metabolism increased in the shPARP-2 cells (Fig. 2D). These genes encompass 1) lipid transport (e.g. fatty acid binding protein-1 (FABP1), microsomal triglyceride transfer protein (MTTP)); 2) lipid modification (e.g. cytochrome P450, family 7, subfamily A, polypeptide 1 (CYP7A1), cytochrome P450, family

39, subfamily A, polypeptide 1 (CYP39A1), fatty acid desaturase 2 (FADS2)) and 3) lipid breakdown (e.g. lipase A (LIPA), endothelial lipase (LIPG), acyl-CoA oxidase 2 (ACOX2)), which is in alignment with decreased hepatic triglyceride storage and enhanced hepatic triglyceride oxidation [5]. Furthermore, we have observed the induction of genes involved in cholesterol biosynthesis: cytosolic 3-hydroxy-3-methylglutaryl (HMG)-CoA synthase (HMGCS1), HMG-CoA reductase (HMGCR), LDL receptor (LDLR), farnesyl diphosphate synthase (FDPS), cytochrome P450, family 51 subfamily A, polypeptide 1 (cyp51A1), stearoyl-CoA delta-9-desaturase (SCD), cetyl-CoA carboxylase alpha (ACACA), fatty acid synthase (FASN), ATP citrate lyase (ACLY), PPARG, and malic enzyme 2 (ME2). In line with these findings HMGCS1 and HMGCR were induced in the livers of PARP-2<sup>-/-</sup> mice (Fig. 2E).

Higher cholesterol levels and the induction of genes of cholesterol synthesis suggested that the knockdown of PARP-2 directly affected transcription factor(s). It was likely that sterol regulatory element-binding proteins (SREBPs), SREBP1 and -2, both responsible for the cholesterol biosynthesis and cholesterol import [19,20], mediated the effect of PARP-2 knockdown on sterol biosynthesis. Upon activation, membrane-bound SREBPs undergo a cascade of proteolytic cleavage leading to their nuclear translocation and transcriptional activation [21,22]. Processed SREBP1 and -2 bind to specific promoters and, in turn, enhance the transcription of genes involved in cholesterol biosynthesis and transport, such as HMGCS, HMGCR, LDLR, FDPS, cytochrome P450, cyp51A1, SCD, ACACA, FASN, ACLY, PPARG and ME2 [21–23]. Our observation that these genes were induced in shPARP-2 HepG2 cells points towards enhanced transactivation by SREBPs.

The induction of SREBP-mediated genes upon the partial deletion of PARP-2 suggested the involvement of SREBP1 and/or SREBP2. Therefore we analyzed the expression of SREBP1 and SREBP2 in scPARP2 and shPARP2 HepG2 cells. We have observed higher expression of SREBP1, but not of SREBP2 in shPARP-2 HepG2 cells (Fig. 3A). In line with these findings, SREBP1 mRNA expression was higher in PARP-2<sup>-/-</sup> mice than in PARP-2<sup>+/+</sup> mice (Fig. 3B). Higher SREBP1 mRNA levels were translated into increased protein levels both in cells and in mice (Figs. 3C, D, S1A, C). We also analyzed the protein expression of two SREBP-dependent genes, HMGCS1 and HMGCR that were induced in both models (Figs. 3C, D, S1B, D).

SREBP1 localization was characterized in HepG2 cells by cell fractionation followed by Western blotting and by confocal microscopy. The full length (unprocessed, cytoplasmic) and cleaved (processed, nuclear) form of SREBP1 protein was higher in shPARP-2 HepG2 cells as shown in cell fractionation experiments (Figs. 3C, S1A). Conforming with these findings, the protein level of the processed form of SREBP1, HMGCS1 and HMGCR was higher in total protein extracts from PARP-2<sup>-/-</sup> mice than in extracts from PARP-2<sup>+/+</sup> mice (Figs. 3D, S1C). Confocal microscopy – performed on scPARP-2 and shPARP-2 HepG2 cells – not only confirmed the above findings, but also revealed that SREBP1 content in the nuclear compartment was higher as compared to the cytoplasm in shPARP-2 HepG2 cells (Fig. 3E). Apparently the partial deletion of PARP-2 induces SREBP1 expression and nuclear translocation suggesting higher SREBP1-mediated transactivation that is translated into higher expression of the genes of cholesterol biosynthesis that likely explains higher cholesterol levels observed in the shPARP-2 HepG2 cells. We did not detect changes in SREBP2 protein levels and localization (data not shown) therefore we omitted it from further investigation.

Higher SREBP1 expression suggests that PARP-2 probably mediates the activity of the promoter of SREBP1. Indeed, the depletion of PARP-

**Fig. 2.** PARP-2 knockdown leads to higher expression of SREBP1-dependent genes. (A–B) PARP-2 mRNA (A) and protein (B) levels were determined in RT-qPCR reactions and Western blots in HepG2 cells treated with PARP-2 specific (shPARP-2), or a non-specific control shRNA (scPARP-2) (n = 6/6). In panel B brightness and contrast were adjusted. (C) Cholesterol content of scPARP-2 and shPARP-2 HepG2 cells (n = 3/3) was extracted by Floch extraction and was determined in colorimetric assays as described in the Materials and methods. (D) Gene expression was analyzed in scPARP-2 and shPARP-2 HepG2 cells (n = 3/3) using microarray as described in the Materials and methods. The result of the analysis was depicted as heatmaps. All abbreviations are in the text. (E) mRNA levels of HMGCS1 and HMGCR (two SREBP target genes) were determined by RT-qPCR in the liver of PARP-2<sup>+/+</sup> and PARP-2<sup>-/-</sup> mice (n = 7/6, age 6 months). \* and \*\*\* indicate statistically significant differences between scPARP-2 HepG2 cells/PARP-2<sup>+/+</sup> mice and shPARP-2 HepG2 cells/PARP-2<sup>-/-</sup> mice at  $p < 0.05$  and  $p < 0.001$ , respectively. In panel E error is given as SEM.

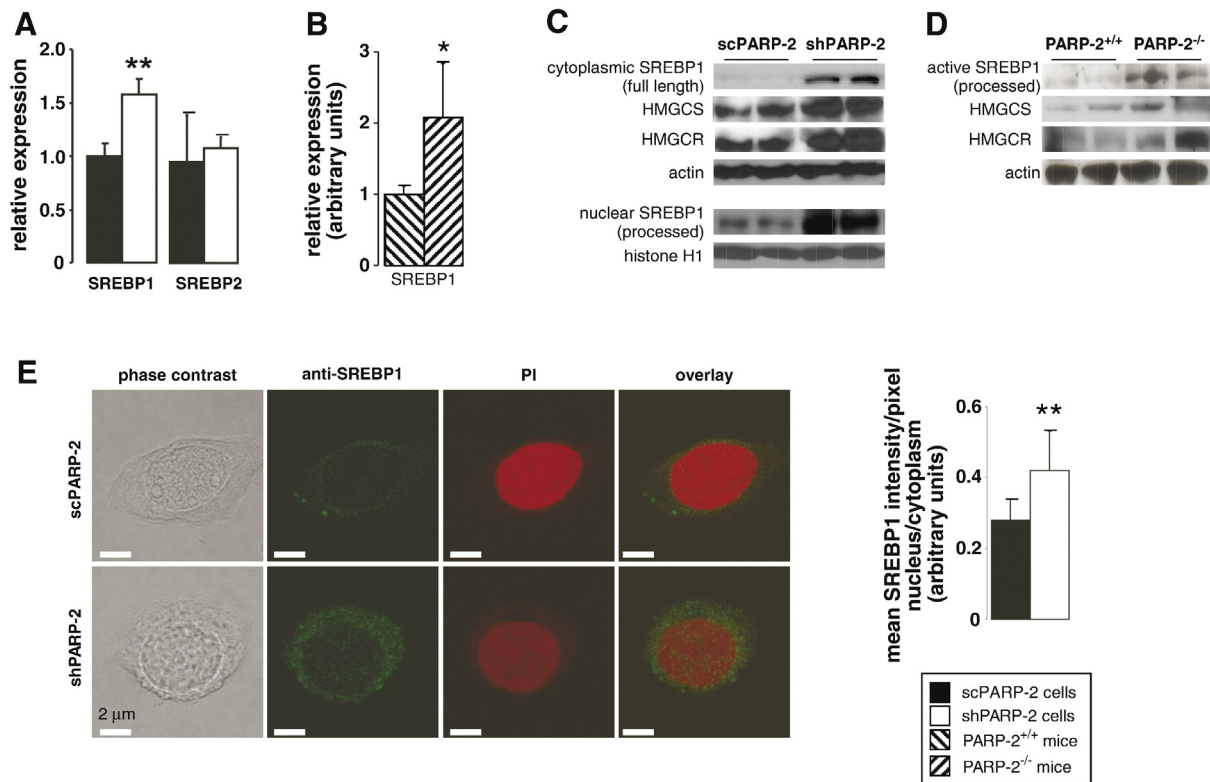


**Fig. 3.** PARP-2 knockdown induces the expression and nuclear accumulation of SREBP1. (A) SREBP1 and -2 mRNA levels were determined in RT-qPCR reactions in scPARP-2 and shPARP-2 HepG2 cells ( $n = 3/3$ ). (B) mRNA levels of SREBP1 were determined by RT-qPCR in the liver of PARP-2<sup>+/+</sup> and PARP-2<sup>-/-</sup> mice ( $n = 7/6$ , age 6 months). (C) scPARP-2 and shPARP-2 HepG2 cells were fractionated ( $n = 3/3$ ) as described in the Materials and methods. Nuclear and cytosolic fractions were analyzed for SREBP1 content by Western blotting. Furthermore, from the cytosolic fraction HMGCS1 and HMGCR were also determined by Western blotting. The results of densitometric analysis are in Fig. S1A–B. (D) Protein levels of SREBP1, HMGCS1 and HMGCR were determined by Western blotting in the liver of PARP-2<sup>+/+</sup> and PARP-2<sup>-/-</sup> mice ( $n = 7/6$ , age 6 months). The results of densitometric analysis are in Fig. S1C–D. (E) Cellular localization of SREBP1 was detected using immunofluorescence staining followed by confocal microscopy in sc PARP-2 and shPARP-2 HepG2 cells, as described in the Materials and methods. Scale bar equals 2  $\mu\text{m}$ . \* and \*\* indicate statistically significant differences between scPARP-2 HepG2 cells/PARP-2<sup>+/+</sup> mice and shPARP-2 HepG2 cells/PARP-2<sup>-/-</sup> mice at  $p < 0.05$  and  $p < 0.01$ , respectively. In panel B error is given as SEM.

2 induced the activity of the promoter of SREBP1 as shown in luciferase reporter assays (Fig. 4A) suggesting that PARP-2 is a repressor of the SREBP1 promoter. Previously it has been shown for numerous promoters that PARP-2 exerts its activity by directly binding to DNA [5,6,14,15,17] that seems likely in the case of the SREBP1 promoter, too. To verify, we performed ChIP assays using an antibody against PARP-2 and oligonucleotide probes for SREBP1 (specific probes for the SREBP1 promoter and SREBP1 coding region) and keratin 19 (K19) promoter (non-PARP-2 dependent promoter, a negative control [6]). In these ChIP assays we found the following:

- 1) PARP-2 is more abundant on the SREBP1 promoter in the scPARP-2 than in the shPARP-2 HepG2 cells reflecting the actual expression levels of PARP-2 (measurements with the anti-PARP-2 antibody and the SREBP1 promoter probe comparing both cell lines; Fig. 4B comparing the first two bars)
- 2) In both cell lines the negative controls of the anti-PARP-2 antibody (nonspecific antibody and the no antibody control) displayed lower signals than the specific anti-PARP-2 antibody (Fig. 4B comparing the black bars).
- 3) The signal of the anti-PARP-2 antibody was lower on the non-specific K19 promoter than on the SREBP1 promoter in scPARP-2 HepG2 cells (Fig. 4B–C comparing black bars on both charts).
- 4) We did not obtain any signal from the coding region of SREBP1 (signal of the anti-PARP-2 antibody using a probe against the SREBP1 coding region; data not shown).

In conclusion, reduced signal of the anti-PARP-2 antibody in shPARP-2 HepG2 cells (detailed above) as compared to the signal in scHepG2 cells from the SREBP1 promoter suggests that the signal of

the anti-PARP-2 antibody is specific and PARP-2 indeed binds to the promoter of SREBP1. It is very likely therefore that the presence of PARP-2 on the SREBP1 promoter suppresses SREBP1 expression by directly binding to the promoter of the SREBP1 gene.

We assessed whether the enzymatic activity of PARP-2 plays role in the regulation of the expression of SREBP1. To that end we treated scPARP-2 and shPARP-2 HepG2 cells with UPF1069, a PARP inhibitor that shows preference towards PARP-2 as compared to PARP-1 and was shown to mimic the action of PARP-2 ablation [24]. Cells were treated with UPF1069 for 24 h without detectable changes in total cellular PARP activity (data not shown). In other words, UPF1069 treatment affected the activity of PARP-2 but not the activity of PARP-1, as PARP-2 represents 10–15% of total cellular PARP activity [2,5,14,25]. We then analyzed the expression of SREBP1 and a selection of SREBP1-mediated genes (HMGCS1, HMGCR, SCD, PPARG and FPDS) in vehicle/UPF1069-treated sc/shPARP-2 HepG2 cells. The treatment of scPARP-2 HepG2 cells resulted in the enhanced expression of SREBP1 and the aforementioned SREBP1-dependent genes (Fig. 4D) suggesting that the enzymatic activity of PARP-2 is important in mediating SREBP1-dependent gene expression. Furthermore, UPF1069 did not cause significant induction of SREBP1 and SREBP1-mediated genes verifying our findings (Fig. 4D) in shPARP-2 HepG2 cells.

### 3.3. Lower HDL levels in PARP-2<sup>-/-</sup> mice are due to the reduced expression of ABCA1

The initial phenotyping of the liver of PARP-2<sup>-/-</sup> mice revealed lower HDL levels (Fig. 1E). Previous studies have linked lower HDL levels to the downregulation of adenosine triphosphate-binding

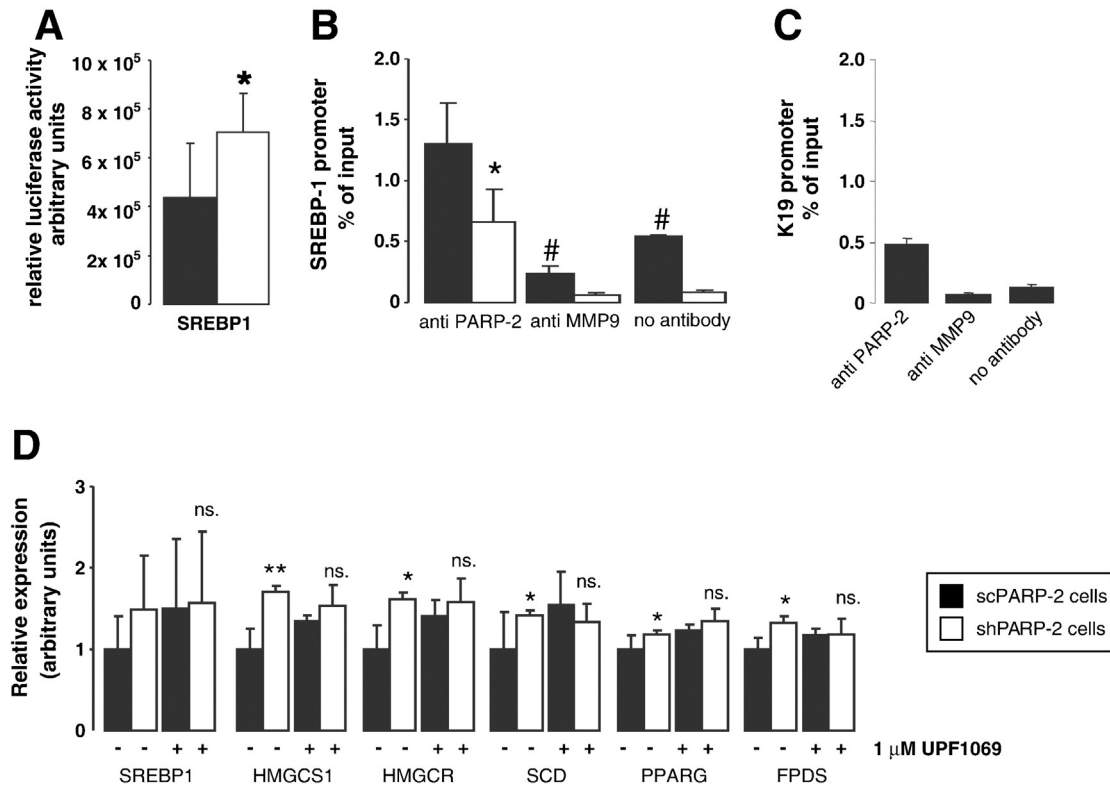


**Fig. 4.** The suppression of the promoter of SREBP1 requires the binding and enzymatic activation of PARP-2. (A) The activity of the promoter of SREBP1 was determined in Luciferase reporter assays in scPARP-2 and shPARP-2 HepG2 cells ( $n = 6/6$ ) as described in the Materials and methods. (B) The promoter occupancy of PARP-2 on the promoter of SREBP1 was determined in ChIP assays in scPARP-2 and shPARP-2 HepG2 cells ( $n = 3/3$ ). (C) The promoter occupancy of PARP-2 on the promoter of K19 (negative control) was assayed in ChIP assays in scPARP-2 HepG2 cells ( $n = 3$ ). (D) scPARP-2 and shPARP-2 HepG2 cells were treated with  $1 \mu\text{M}$  UPF1069 or vehicle ( $n = 6/6/6/6$ ) for 24 h, then RNA was isolated and RT-qPCR analysis was performed with probes specific for the genes indicated. \* and \*\* indicate statistically significant differences between scPARP-2 and shPARP-2 HepG2 cells at  $p < 0.05$  and  $p < 0.01$ , respectively. # indicates statistically significant difference between the signal of anti-PARP-2 antibody vs. anti-MMP9 antibody or no antibody samples at  $p < 0.05$ . "ns." stands for no statistically significant difference between UPF1069-treated scPARP-2 and shPARP-2 HepG2 cells. All abbreviations are in the text.

385 cassette transporter A1 (ABCA1) transporter [26,27], therefore we  
 386 analyzed mRNA and protein levels of ABCA1 in HepG2 cells and  
 387 in mice. ABCA1 mRNA and protein levels decreased upon the deletion  
 388 of PARP-2 in HepG2 cells (Figs. 5A, S2A) and in mice (Figs. 5B, S2B).

To explain the downregulation of ABCA1 expression we analyzed the  
 389 activity of the promoter of ABCA1 upon the deletion of PARP-2, however  
 390 we were unable to show repression in the activity of the promoter upon  
 391 the ablation of PARP-2 (data not shown).  
 392

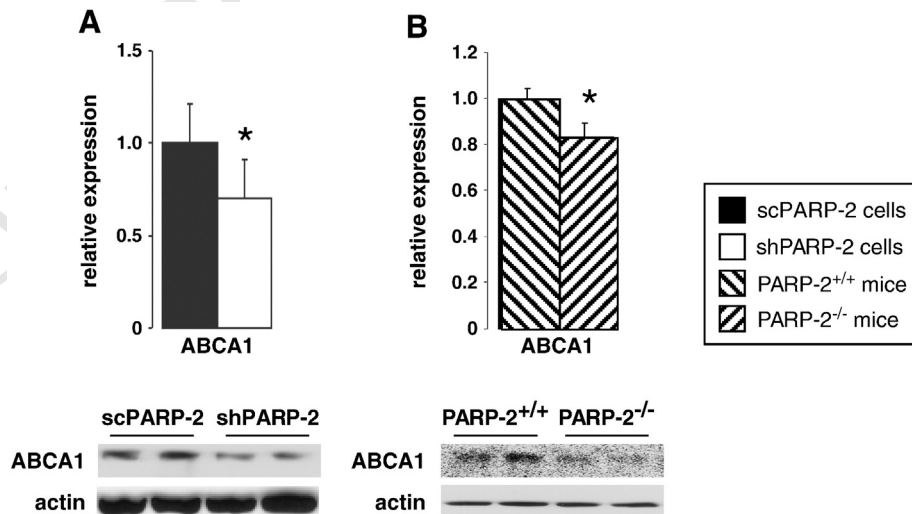


**Fig. 5.** PARP-2 deletion reduces ABCA1 expression in cells and in vivo. (A) The mRNA and protein expression ABCA1 was determined in RT-qPCR reactions by Western blotting in scPARP-2 and shPARP-2 HepG2 cells ( $n = 6/6$ ). (B) The mRNA and protein expression ABCA1 was determined in RT-qPCR reactions by Western blotting in PARP-2<sup>+/+</sup> and PARP-2<sup>-/-</sup> mice ( $n = 6/6$ ) ( $n = 7/6$ , age 6 months). On the Western blot image the brightness and contrast were adjusted. \* indicates statistically significant difference between PARP-2<sup>+/+</sup> mice or scPARP-2 cells and PARP-2<sup>-/-</sup> mice or shPARP-2 cells at  $p < 0.05$ . Error is given as SEM in panel B.

## 4. Discussion

In the present study we have extended the role of PARP-2 in lipid metabolism showing that PARP-2 impacts on cholesterol homeostasis. The deletion of PARP-2 induced cholesterol levels in the liver and decreased serum HDL levels. To identify the underlying molecular mechanism we performed microarray studies, whereby we revealed the dysregulation of 616 genes, although fold changes in expression levels were limited (roughly around  $\pm 2$ –2.5 fold). Previous studies have linked PARP-2 to transcriptional regulation [5–7,14–18,28,29]. Moreover, a recent study showed differences in gene expression between bone marrow cells of PARP-2<sup>+/+</sup> and PARP-2<sup>-/-</sup> mice upon gamma irradiation [29]. However, such widespread rearrangement of gene expression in unchallenged cells upon the depletion of PARP-2 was unexpected. We have identified new groups of genes linked to the expression of PARP-2 (hepatic secretory activity and cholesterol biosynthesis) in addition to the previously known groups (SIRT1-regulated genes, lipid metabolism genes, cell death genes and surfactant protein B) [5–7,15–18].

PARP-2 associates with numerous transcription factors, among them nuclear receptors [e.g. estrogen receptor (ER) $\alpha$  and PPARs] as reviewed in [4]. Not surprisingly, studies have already linked PARP-2 to epigenetic regulation that is a likely mode of action for PARP-2 in the regulation of gene expression. Quenet et al. [30] have shown that PARP-2 interacts with tripartite motif containing 28 (TIF1 $\beta$ ) and heterochromatin protein (HP)1 $\alpha$  inducing condensation to heterochromatin. Furthermore, Liang et al. [17] recently found that the presence of PARP-2 enhances the recruitment of histone deacetylase (HDAC)5 and HDAC7 and the histone methyltransferase G9a to promoters. In the same study Liang et al. [17] reported that the suppression of gene expression exerted by PARP-2 was independent of the enzymatic activation of PARP-2. Hereby, we have shown that the inhibition of PARP-2 by UPF1069 had similar effect as the knockdown of PARP-2 suggesting that – at least for SREBP1 – the enzymatic activity of PARP-2 is crucial for the suppression of the promoter. What causes the discrepancy between these studies? Liang et al. [17] utilized genetic tools to assess the activity of PARP-2, while we applied pharmacological means. On the one hand UPF1069 is not a highly specific PARP-2 inhibitor (it shows 60-fold preference towards PARP-2, as compared to PARP-1 in vitro), therefore it cannot be excluded that UPF1069 may inhibit other PARP enzymes as well [24,31]. Another explanation is that PARP-2 inhibits certain promoters in a poly(ADP-ribose)-dependent, while others in a poly(ADP-ribose)-independent way. At that point it's impossible to make a definitive selection between these explanations. However, it is important to note that the activity-dependent regulation of gene expression may provide means for pharmacological intervention.

These data provide a likely explanation for the upregulation of certain genes upon the knockdown of PARP-2 (~25% of all dysregulated genes), but does not explain the molecular mechanism through which the majority of genes (~75%) are downregulated under the same condition. It is likely that PARP-2 could act through similar molecular mechanisms as PARP-1 (see [32,33]) to mediate gene expression. Therefore, by analogy with PARP-1, in the future it might be possible to explain how PARP-2 can act as a positive transcriptional cofactor.

By analyzing changes in the expression of the lipid metabolism genes, we found that PARP-2 is a suppressor of the SREBP1 promoter. The knockdown of PARP-2 therefore probably induces SREBP1 expression that leads to cholesterol synthesis and import culminating in cholesterol accumulation. Our data, therefore, identify PARP-2 as a suppressor of SREBP1 expression, similarly to early growth response protein-1 (EGR-1) or FOXO1 [34,35].

Excess hepatic cholesterol was expected to be exported from the liver leading to elevated serum and fecal cholesterol or LDL levels, but this could not be observed. Moreover, to our surprise, serum HDL levels were significantly reduced in the PARP-2<sup>-/-</sup> mice. This unexpected finding is likely explained by the decreased expression of ABCA1

transport protein that is essential in transferring cholesterol to apolipoprotein A1 in the liver and the intestine [26,27,36]. Defect in ABCA1 function manifests in humans as the Tangier disease, that is characterized by decrease in HDL levels and higher risk for atherosclerosis and its sequelae [26,27,37,38]. Therefore lower ABCA1 expression seems to explain decreased HDL levels in PARP-2<sup>-/-</sup> mice. The actual molecular mechanism through which the deletion of PARP-2 leads to lower expression of ABCA1 remains to be explored, although we have excluded the direct action of PARP-2 on the promoter of ABCA1.

Apparently PARP-2 has widespread effects on lipid homeostasis. Upon the depletion of PARP-2 triglyceride storage is reduced in the WAT and liver [5,6], while triglyceride oxidation is enhanced in skeletal muscle and liver [5]. Here we show that the depletion of PARP-2 enhances hepatic cholesterol synthesis and decreases HDL synthesis. As a result, serum free fatty acid, triglyceride and HDL levels are reduced, while LDL levels do not change in PARP-2<sup>-/-</sup> mice. Low HDL levels represent a risk factor to several cardiovascular diseases [39,40]. Interestingly, the depletion of another member of the PARP superfamily, PARP-1 protects from several cardiovascular diseases [41–46]. It might be possible that PARP-1 and PARP-2 have different and, at some points, opposing effects in predisposing to cardiovascular diseases that may necessitate further research efforts in that direction.

Supplementary data to this article can be found online at <http://dx.doi.org/10.1016/j.bbadis.2013.12.006>.

## Acknowledgement

We acknowledge the help of Drs. Bálint L. Bálint and Szilárd Pólska (UD Genomed, Debrecen, Hungary) in microarray experiments, Dr. György Haskó (UMDNJ, NJ, USA) for critically revising the text, Dr. László Nagy (University of Debrecen) in advising manuscript organization and the technical assistance of Mrs. Erzsébet Herbály and László Gelenczey-Finta.

This work was supported by National Innovation Office [Seahorse grant], TÁMOP-4.2.2/B-10/1-2010-0024, TÁMOP-4.2.2.A-11/1/KONV-2012-0025, TÁMOP-4.2.1./B-09/KONV-2010-0007, TÁMOP 4.2.4. A/2-11-1-2012-0001, OTKA [CNK80709, PD83473, K77600, K103965, K108308], and University of Debrecen [Mecenatura Mec-8/2011]. PB and SM are recipients of Bolyai fellowship from the Hungarian Academy of Sciences.

Conflict of interest: none declared.

Database linking: Raw and processed data of the microarray experiment is uploaded to NCBI GEO (accession No. 16716091).

## References

- J.C. Ame, V. Rolli, V. Schreiber, C. Niedergang, F. Apiou, P. Decker, S. Muller, T. Hoger, J. Menissier-de Murcia, G. de Murcia, PARP-2, A novel mammalian DNA damage-dependent poly(ADP-ribose) polymerase, *J. Biol. Chem.* 274 (1999) 17860–17868.
- V. Schreiber, J.C. Ame, P. Dolle, I. Schultz, B. Rinaldi, V. Fraulob, J. Menissier-de Murcia, G. de Murcia, Poly(ADP-ribose) polymerase-2 (PARP-2) is required for efficient base excision DNA repair in association with PARP-1 and XRCC1, *J. Biol. Chem.* 277 (2002) 23028–23036.
- S.S. Haenni, P.O. Hassa, M. Altmeyer, M. Fey, R. Imhof, M.O. Hottiger, Identification of lysines 36 and 37 of PARP-2 as targets for acetylation and auto-ADP-ribosylation, *Int. J. Biochem. Cell Biol.* 40 (2008) 2274–2283.
- M. Szanto, A. Brunyánszki, B. Kiss, L. Nagy, P. Gergely, L. Virag, P. Bai, Poly(ADP-ribose) polymerase-2: emerging transcriptional roles of a DNA repair protein, *Cell. Mol. Life Sci.* 69 (2012) 4079–4092.
- P. Bai, C. Canto, A. Brunyánszki, A. Huber, M. Szanto, Y. Cen, H. Yamamoto, S.M. Houten, B. Kiss, H. Oudart, P. Gergely, J. Menissier-de Murcia, V. Schreiber, A.A. Sauve, J. Auwerx, PARP-2 regulates SIRT1 expression and whole-body energy expenditure, *Cell Metab.* 13 (2011) 450–460.
- P. Bai, S.M. Houten, A. Huber, V. Schreiber, M. Watanabe, B. Kiss, G. de Murcia, J. Auwerx, J. Menissier-de Murcia, Poly(ADP-ribose) polymerase-2 controls adipocyte differentiation and adipose tissue function through the regulation of the activity of the retinoid X receptor/peroxisome proliferator-activated receptor-gamma heterodimer, *J. Biol. Chem.* 282 (2007) 37738–37746.
- Y. Maeda, T.C. Hunter, D.E. Loudy, V. Dave, V. Schreiber, J.A. Whitsett, PARP-2 interacts with TTF-1 and regulates expression of surfactant protein-B, *J. Biol. Chem.* 281 (2006) 9600–9606.

- 526 [8] P. Bai, C. Canto, The role of PARP-1 and PARP-2 enzymes in metabolic regulation and  
527 disease, *Cell Metab.* 16 (2012) 290–295.
- 528 [9] S. Erener, A. Mirsaidi, M. Hesse, A.N. Tiaden, H. Ellingsgaard, R. Kostadinova, M.Y.  
529 Donath, P.J. Richards, M.O. Hottiger, ARTD1 deletion causes increased hepatic lipid  
530 accumulation in mice fed a high-fat diet and impairs adipocyte function and differ-  
531 entiation, *Faseb J.* 26 (2012) 2631–2638.
- 532 [10] P. Bai, C. Canto, H. Oudart, A. Brunyanszki, Y. Cen, C. Thomas, H. Yamamoto, A.  
533 Huber, B. Kiss, R.H. Houtkooper, K. Schoonjans, V. Schreiber, A.A. Sauve, J.  
534 Menissier-de Murcia, J. Auwerx, PARP-1 inhibition increases mitochondrial metabo-  
535 lism through SIRT1 activation, *Cell Metab.* 13 (2011) 461–468.
- 536 [11] J. Menissier-de Murcia, M. Ricoul, L. Tartier, C. Niedergang, A. Huber, F. Dantzer, V.  
537 Schreiber, J.C. Ame, A. Dierich, M. LeMeur, L. Sabatier, P. Chambon, G. de Murcia,  
538 Functional interaction between PARP-1 and PARP-2 in chromosome stability and  
539 embryonic development in mouse, *EMBO J.* 22 (2003) 2255–2263.
- 540 [12] K. Erdelyi, P. Bai, I. Kovacs, E. Szabo, G. Mocsar, A. Kakuk, C. Szabo, P. Gergely, L.  
541 Virag, Dual role of poly(ADP-ribose) glycohydrolase in the regulation of cell death  
542 in oxidatively stressed A549 cells, *Faseb J.* 23 (2009) 3553–3563.
- 543 [13] A.H. Hasty, H. Shimano, N. Yahagi, M. Amemiya-Kudo, S. Perrey, T. Yoshikawa, J.  
544 Osuga, H. Okazaki, Y. Tamura, Y. Iizuka, F. Shionoiri, K. Ohashi, K. Harada, T. Gotoda,  
545 R. Nagai, S. Ishibashi, N. Yamada, Sterol regulatory element-binding protein-1 is regu-  
546 lated by glucose at the transcriptional level, *J. Biol. Chem.* 275 (2000) 31069–31077.
- 547 [14] M. Szanto, I. Rutkai, C. Hegedus, A. Czizkora, M. Rozsahegyi, B. Kiss, L. Virag, P. Gergely, A.  
548 Toth, P. Bai, Poly(ADP-ribose) polymerase-2 depletion reduces doxorubicin-induced  
549 damage through SIRT1 induction, *Cardiovasc. Res.* 92 (2011) 430–438.
- 550 [15] B. Geng, Y. Cai, S. Gao, J. Lu, L. Zhang, J. Zou, M. Liu, S. Yu, J. Ye, P. Liu, PARP-2 knock-  
551 down protects cardiomyocytes from hypertrophy via activation of SIRT1, *Biochem.*  
552 *Biophys. Res. Commun.* 430 (2013) 944–950.
- 553 [16] J. Yelamos, Y. Monreal, L. Saenz, E. Aguado, V. Schreiber, R. Mota, T. Fuente, A.  
554 Minguela, P. Parrilla, G. de Murcia, E. Almarza, P. Aparicio, J. Menissier-de Murcia,  
555 PARP-2 deficiency affects the survival of CD4<sup>+</sup>CD8<sup>+</sup> double-positive thymocytes,  
556 *EMBO J.* 25 (2006) 4350–4360.
- 557 [17] Y.C. Liang, C.Y. Hsu, Y.L. Yao, W.M. Yang, PARP-2 regulates cell cycle-related genes  
558 through histone deacetylation and methylation independently of poly(ADP-ribosyl)  
559 ation, *Biochem. Biophys. Res. Commun.* 431 (2013) 58–64.
- 560 [18] O. Cohausz, F.R. Althaus, Role of PARP-1 and PARP-2 in the expression of  
561 apoptosis-regulating genes in HeLa cells, *Cell Biol. Toxicol.* 25 (2008) 379–391.
- 562 [19] M.S. Brown, J.L. Goldstein, The SREBP pathway: regulation of cholesterol metabolism  
563 by proteolysis of a membrane-bound transcription factor, *Cell* 89 (1997) 331–340.
- 564 [20] J.D. Horton, N.A. Shah, J.A. Warrington, N.N. Anderson, S.W. Park, M.S. Brown, J.L.  
565 Goldstein, Combined analysis of oligonucleotide microarray data from transgenic  
566 and knockout mice identifies direct SREBP target genes, *Proc. Natl. Acad. Sci. U. S.*  
567 *A.* 100 (2003) 12027–12032.
- 568 [21] X. Wang, R. Sato, M.S. Brown, X. Hua, J.L. Goldstein, SREBP-1, a membrane-bound  
569 transcription factor released by sterol-regulated proteolysis, *Cell* 77 (1994) 53–62.
- 570 [22] X. Hua, C. Yokoyama, J. Wu, M.R. Briggs, M.S. Brown, J.L. Goldstein, X. Wang, SREBP-2,  
571 a second basic-helix-loop-helix-leucine zipper protein that stimulates transcription  
572 by binding to a sterol regulatory element, *Proc. Natl. Acad. Sci. U. S. A.* 90 (1993)  
573 11603–11607.
- 574 [23] J.D. Horton, I. Shimomura, S. Ikemoto, Y. Bashmakov, R.E. Hammer, Overexpression  
575 of sterol regulatory element-binding protein-1a in mouse adipose tissue produces  
576 adipocyte hypertrophy, increased fatty acid secretion, and fatty liver, *J. Biol. Chem.*  
577 278 (2003) 36652–36660.
- 578 [24] F. Moroni, L. Formentini, E. Gerace, E. Camaioni, D.E. Pellegrini-Giampietro, A.  
579 Chiarugi, R. Pellicciari, Selective PARP-2 inhibitors increase apoptosis in hippocam-  
580 pal slices but protect cortical cells in models of post-ischaemic brain damage, *Br. J.*  
581 *Pharmacol.* 157 (2009) 854–862.
- 582 [25] W.M. Shieh, J.C. Ame, M.V. Wilson, Z.Q. Wang, D.W. Koh, M.K. Jacobson, E.L.  
583 Jacobson, Poly(ADP-ribose) polymerase null mouse cells synthesize ADP-ribose  
584 polymers, *J. Biol. Chem.* 273 (1998) 30069–30072.
- 585 [26] M. Bodzioch, E. Orso, J. Klucken, T. Langmann, A. Böttcher, W. Diederich, W. Drobniak,  
586 S. Barlage, C. Buchler, M. Porsch-Ozcurumez, W.E. Kaminski, H.W. Hahmann, K. Oette,  
587 G. Rothe, C. Aslanidis, K.J. Lackner, G. Schmitz, The gene encoding ATP-binding  
588 cassette transporter 1 is mutated in Tangier disease, *Nat. Genet.* 22 (1999) 347–351.
- [27] A. Brooks-Wilson, M. Marcil, S.M. Clee, L.H. Zhang, K. Roomp, M. van Dam, L. Yu, C. 589  
Brewer, J.A. Collins, H.O. Molhuizen, O. Loubser, B.F. Ouellette, K. Fichter, K.J. 590  
Ashbourne-Excoffon, C.W. Sensen, S. Scherer, S. Mott, M. Denis, D. Martindale, J. 591  
Frohlich, K. Morgan, B. Koop, S. Pimstone, J.J. Kastelein, J. Genest Jr., M.R. Hayden, 592  
Mutations in ABC1 in Tangier disease and familial high-density lipoprotein deficiency, 593  
*Nat. Genet.* 22 (1999) 336–345.
- [28] V.S. Meder, M. Boeglin, G. de Murcia, V. Schreiber, PARP-1 and PARP-2 interact with 595  
nucleophosmin/B23 and accumulate in transcriptionally active nucleoli, *J. Cell Sci.* 596  
118 (2005) 211–222.
- [29] J. Farres, J. Martin-Caballero, C. Martinez, J.J. Lozano, L. Llacuna, C. Ampurdanes, C. 598  
Ruiz-Herguido, F. Dantzer, V. Schreiber, A. Villunger, A. Bigas, J. Yelamos, PARP-2 is 599  
required to maintain hematopoiesis following sublethal gamma-irradiation in 600  
mice, *Blood* 122 (2013) 44–54.
- [30] D. Quenet, V. Gasser, L. Fouillen, F. Cammas, S. Sanglier-Cianferani, R. Losson, F. 602  
Dantzer, The histone subcode: poly(ADP-ribose) polymerase-1 (Parp-1) and 603  
Parp-2 control cell differentiation by regulating the transcriptional intermediary 604  
factor TIF1beta and the heterochromatin protein HP1alpha, *Faseb J.* 22 (2008) 605  
3853–3865.
- [31] E. Wahlberg, T. Karlberg, E. Kouznetsova, N. Markova, A. Macchiarulo, A.G. Thorsell, 607  
E. Pol, A. Frostell, T. Ekblad, D. Oncu, B. Kull, G.M. Robertson, R. Pellicciari, H. Schuler, 608  
J. Weigelt, Family-wide chemical profiling and structural analysis of PARP and 609  
tanyrase inhibitors, *Nat. Biotechnol.* 30 (2012) 283–288.
- [32] W.L. Kraus, Transcriptional control by PARP-1: chromatin modulation, enhancer- 611  
binding, coregulation, and insulation, *Curr. Opin. Cell Biol.* 20 (2008) 294–302. 612
- [33] W.L. Kraus, M.O. Hottiger, PARP-1 and gene regulation: progress and puzzles, *Mol.* 613  
*Aspects Med.* 34 (2013) 1109–1123. 614
- [34] X. Liu, A. Qiao, Y. Ke, X. Kong, J. Liang, R. Wang, X. Ouyang, J. Zuo, Y. Chang, F. Fang, 615  
FoxO1 represses LX $\alpha$ -mediated transcriptional activity of SREBP-1c promoter in 616  
HepG2 cells, *FEBS Lett.* 584 (2010) 4330–4334. 617
- [35] A. Fernandez-Alvarez, G. Tur, G. Lopez-Rodas, M. Casado, Reciprocal regulation of 618  
the human sterol regulatory element binding protein (SREBP)-1a promoter by 619  
Sp1 and EGR-1 transcription factors, *FEBS Lett.* 582 (2008) 177–184. 620
- [36] F.J. Field, K. Watt, S.N. Mathur, Origins of intestinal ABCA1-mediated 621  
HDL-cholesterol, *J. Lipid Res.* 49 (2008) 2605–2619. 622
- [37] G.D. Kolovou, D.P. Mikhailidis, K.K. Anagnostopoulou, S.S. Daskalopoulou, D.V. 623  
Cokkinos, Tangier disease four decades of research: a reflection of the importance 624  
of HDL, *Curr. Med. Chem.* 13 (2006) 771–782. 625
- [38] M.H. Kang, R. Singaraja, M.R. Hayden, Adenosine-triphosphate-binding cassette 626  
transporter-1 trafficking and function, *Trends Cardiovasc. Med.* 20 (2010) 41–49. 627
- [39] H. Soran, S. Hama, R. Yadav, P.N. Durrington, HDL functionality, *Curr. Opin. Lipidol.* 628  
23 (2012) 353–366. 629
- [40] E.A. Fisher, J.E. Feig, B. Hewing, S.L. Hazen, J.D. Smith, High-density lipoprotein func- 630  
tion, dysfunction, and reverse cholesterol transport, *Arterioscler. Thromb. Vasc. Biol.* 631  
32 (2012) 2813–2820. 632
- [41] P. Pacher, J.S. Beckman, L. Liaudet, Nitric oxide and peroxynitrite in health and 633  
disease, *Physiol. Rev.* 87 (2007) 315–424. 634
- [42] P. Pacher, L. Liaudet, P. Bai, L. Virag, J.G. Mabley, G. Hasko, C. Szabo, Activation of 635  
poly(ADP-ribose) polymerase contributes to development of doxorubicin-induced 636  
heart failure, *J. Pharmacol. Exp. Ther.* 300 (2002) 862–867. 637
- [43] C.P. Hans, Y. Feng, A.S. Naura, M. Zerfaoui, B.M. Rezk, H. Xia, A.D. Kaye, K. Matrougui, 638  
E. Lazartigues, A.H. Boulares, Protective effects of PARP-1 knockout on 639  
dyslipidemia-induced autonomic and vascular dysfunction in ApoE mice: effects 640  
on eNOS and oxidative stress, *PLoS One* 4 (2009) e7430. 641
- [44] C.P. Hans, M. Zerfaoui, A.S. Naura, A. Catling, A.H. Boulares, Differential effects of 642  
PARP inhibition on vascular cell survival and ACAT-1 expression favouring athero- 643  
sclerotic plaque stability, *Cardiovasc. Res.* 78 (2008) 429–439. 644
- [45] R. Benko, P. Pacher, A. Vaslin, M. Kollai, C. Szabo, Restoration of the endothelial 645  
function in the aortic rings of apolipoprotein E deficient mice by pharmacological 646  
inhibition of the nuclear enzyme poly(ADP-ribose) polymerase, *Life Sci.* 75 (2004) 647  
1255–1261. 648
- [46] S. Xu, P. Bai, P.J. Little, P. Liu, Poly(ADP-ribose) polymerase 1 (PARP1) in 649  
atherosclerosis: from molecular mechanisms to therapeutic implications, *Mol.* 650  
*Med. Rev.* (2013), <http://dx.doi.org/10.1002/med.21300>. 651  
652